Die Rolle der Dual Energy-Computertomographie bei der Abklärung von Nebennierenraumforderungen sowie in der Überwachung von antiangiogenetischen Therapiekonzepten

München 2018

Aus der Klinik und Poliklinik für Radiologie
der
Ludwig-Maximilians-Universität München

Direktor: Prof. Dr. med. Jens Ricke

Die Rolle der Dual Energy-Computertomographie bei der Abklärung von Nebennierenraumforderungen sowie in der Überwachung von antiangiogenetischen Therapiekonzepten

Dissertation
zum Erwerb des Doktorgrades der Medizin
an der Medizinischen Fakultät der
Ludwig-Maximilians-Universität zu München

vorgelegt von
Nicolai Hummel

aus Schramberg

München 2018

Mit Genehmigung der Medizinischen Fakultät der Universität München

Berichterstatter:	Prof. Dr. med. Anno Graser
Mitberichterstatter:	Prof. Dr. med. Ulrich-Georg Fink
	Prof. Dr. med. Martin Reincke
Mitbetreuung durch den promovierten Mitarbeiter:	Prof. Dr. med. Andreas Dietrich Helck
Dekan:	Prof. Dr. med. dent. Reinhard Hickel
Tag der mündlichen Prüfung:	21.06.2018

Eidesstattliche Versicherung

Hummel, Nicolai

Name, Vorname

Ich erkläre hiermit an Eides statt,

dass ich die vorliegende Dissertation mit dem Thema “Die Rolle der Dual Energy-Computertomographie bei der Abklärung von Nebennierenraumforderungen sowie in der Überwachung von antiangiogenetischen Therapiekonzepten” selbständig verfasst, mich außer der angegebenen keiner weiteren Hilfsmittel bedient und alle Erkenntnisse, die aus dem Schrifttum ganz oder annähernd übernommen sind, als solche kenntlich gemacht und nach ihrer Herkunft unter Bezeichnung der Fundstelle einzeln nachgewiesen habe.

Ich erkläre des Weiteren, dass die hier vorgelegte Dissertation nicht in gleicher oder in ähnlicher Form bei einer anderen Stelle zur Erlangung eines akademischen Grades eingereicht wurde.

29.06.2018 — Ort, Datum

N. Hummel — Unterschrift Doktorandin/Doktorand

Inhaltsverzeichnis

1 Abkürzungsverzeichnis

CT	Computertomographie
CTDI	Dosis Index für CT
DECT	Dual-Energy-Computertomographie
DLP	Dosislängenprodukt
HU	Houndsfield-Einheiten
ID	Iodine - related - density
keV	Kiloelektronenvolt
MRT	Magneteresonanz-Tomographie
NCC	Nierenzellkarzinom
PET	Positronen-Emissions-Tomographie
TKI	Tyrosin-Kinase-Inhibitoren
VNC	Virtual non-contrast image

2 Publikationsliste

1. A. Helck, N. Hummel (contributed equally) et. al.: „Can single-phase dual-energy CT reliably identify adrenal adenomas?", European Radiology, Juli 2014, Seiten 1636 - 1642, PubMed PMID: 24804633.

2. K. Hellbach, N. Hummel et. al.: „Dual energy CT allows for improved characterization of response to antiangiogenic treatment in patients with metastatic renal cell cancer ", European Radiology, September 2016, Seiten 2532 - 2537, PubMed PMID: 27678131.

3 Einleitung

3.1 Forschungsvorhaben

Der Stellenwert der Computertomographie (CT) als diagnostisches Verfahren nimmt in der modernen Medizin stetig zu, was sich auch in seit Jahren deutlich steigenden Untersuchungszahlen widerspiegelt. So nahm beispielsweise die Anzahl der durchgeführten Computertomographien im Zeitraum von 2006 bis 2012 um circa 130 Prozent zu. (1)

Die diagnostische Aussagekraft dieser häufig eingesetzten Untersuchung zu optimieren ist somit von hoher klinischer Relevanz. Hierfür bietet die neuartige Dual-Energy-CT-Technologie mit ihren softwarebasierten Nachbearbeitungsmöglichkeiten (post-processing) vielversprechende Möglichkeiten. Zwei Anwendungen, nämlich die Erstellung von virtuellen Nativbildern und die Jod-Quantifizierung, wurden in den vorliegenden Forschungsarbeiten näher untersucht.

3.2 Dual-Energy-Computertomographie

Bei einem Dual-Source-Computertomographen rotieren gleichzeitig zwei in einem 90°-Winkel montierte Röntgenröhren um den Patienten. Jeweils gegenüberliegend finden sich die korrespondierenden Detektoren. Ein herkömmlicher Computertomograph ist im Gegensatz hierzu mit lediglich einer Röntgenstrahlungsquelle ausgestattet (siehe Abbildung 1).

Ein wesentlicher Vorteil ist dabei, dass gleichzeitig Datensätze mit unterschiedlichen Röhrenspannungen erhoben werden können. Dies ermöglicht erst die Anwendungen, die in den nachfolgenden Publikationen untersucht wurden. Daneben können die beiden Röntgenstrahler auch mit der gleichen Röhrenspannung betrieben werden, was beispielsweise Vorteile bei der Diagnostik adipöser Patienten oder auch bei kardiovaskulärer Bildgebung bietet (2).

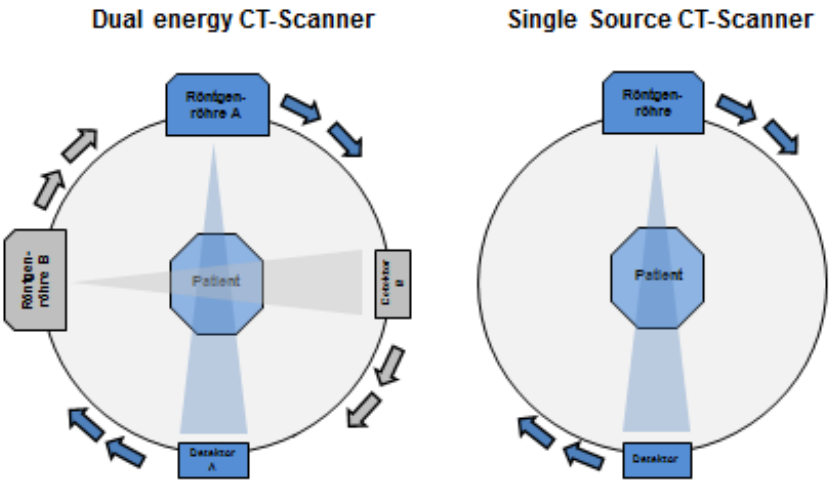

Abbildung 1: Anordnung der Röntgenröhren und der Detektoren bei DECT-Scannern sowie bei CT-Scannern

3.3 Physikalische Grundlagen

In der Röntgenröhre werden mit einer Glühkathode freie Elektronen erzeugt. Mittels einer zwischen Kathode und Anode angelegten Spannung werden die Elektronen in Richtung Anode beschleunigt. Die Elektronen erhalten hierdurch kinetische Energie. Diese wird beim Auftreffen auf die Anode überwiegend in Form von Wärme frei. Circa ein Prozent der Energie wird in Form von Bremsstrahlung freigesetzt. Hierbei handelt es sich um kurzwellige elektromagnetische Strahlung, welche ein kontinuierliches Intensitätsspektrum aufweist.

Die an der Röntgenröhre angelegte Spannung beeinflusst den Energiegehalt des entsandten Röntgenphotons. Umso niedriger die Röhrenspannung, desto niedriger das Spektrum der Energielevels der entsandten Photonen.

Die Strahlenabschwächung, welche Röntgenstrahlung beim Auftreffen auf ein Atom erfährt, ist wiederum unter anderem von der Energie des einfallenden Röntgenphotons abhängig.

Ferner beeinflusst die Ordnungszahl des bestrahlten Atoms (und damit die

Bindungsenergie zwischen Atomkern und kernnahen Elektronen) die Wahrscheinlichkeit des Auftretens des photoelektrischen Effekts und hierdurch die Intensität der Strahlenabschwächung.

Überschreitet die Energie des einfallenden Photons diese Bindungsenergie lediglich in geringem Maße, so kommt es zu einer Absorptionsspitze (K-Kante). Je näher die Energie des Photons der K-Kante des bestrahlten Atoms ist, desto stärker die Strahlenabschwächung. (3)

CT-Kontrastmittel enthalten eine relativ hohe Konzentration von Jod. Der spezifische K-edge von diesen Jod-Atomen liegt bei 33,2 keV.

Die Absorption durch Iod-Atome ist somit bei einer Bestrahlung mit einer mit 80 keV erzeugten Röntgenstrahlung stärker als bei einer Bestrahlung mit einer Röhrenspannung von 140 keV.

Durch Bestrahlung eines Materials mit Photonen, welche bei unterschiedlichen Röhrenspannungen generiert wurden, können somit Rückschlüsse auf dessen Iod-Gehalt gezogen werden.

3.4 Virtuelle Nativbilder (virtual non-contrast-images, VNC)

Im Rahmen des post-processing werden in einer Kontrastmittelphase aufgenommene Bildserien nachbearbeitet. Das im untersuchten Gewebe enthaltene Iod-haltige Kontrastmittel kann digital aus dem Bild subtrahiert werden. Mittels spezieller Software (in den vorliegenden Studien Syngo.via “CT Dual Energy“, Siemens Healthcare) gelingt es also, aus kontrastmittelverstärkten CT-Bildern virtuelle Nativbilder (virtual non-contrast images) zu erstellen.

Somit kann dann auf die zusätzliche Anfertigung einer Nativ-CT-Serie verzichtet werden.

3.5 Iodine related density (ID)

Ferner besteht die Möglichkeit aus kontrastmittelverstärkten Bildserien sogenannte „iodine-only“ Bildserien zu erstellen. Hierbei werden lediglich durch Iod erzeugte Bildpunkte dargestellt, während die durch das übrige Gewebe erzeugten Bildpunkte digital entfernt werden. Die auf diese Weise erzeugten Iod-Maps erlauben eine exakte Messung der Kontrastmittelmenge in einer bestimmten Region (Jod-Quantifizierung).

3.6 Übergeordnete Fragestellung

Die auf der Möglichkeit der Iod-Detektion mittels DECT basierenden Werkzeuge „ID“ und „VNC“ finden Anwendung in den beiden vorliegenden Veröffentlichungen.

Beide Studien untersuchen die Vorteile dieser neuartigen diagnostischen Möglichkeiten anhand spezieller Fragestellungen der onkologischen Radiologie.

Die Arbeit mit dem Titel „Can single-phase dual-energy CT reliably identify adrenal adenomas?“ untersucht die Möglichkeit der Differenzierung adrenaler Inzidentalome mittels virtuell generierter Nativbilder (VNC).

In der Studie „Dual energy CT allows for improved characterization of response to antiangiogenic treatment in patients with metastatic renal cell cancer “ werden anhand der Joddichte (ID) sogenannte Jodkarten erstellt und damit die Kontrastmittelaufnahme bei stark vaskularisierten Metastasen des Nierenzell-karzinoms quantifiziert.

3.7 Arbeitsanteil an den Veröffentlichungen

Für die vorliegende Veröffentlichung mit dem Titel „Can single-phase dual-energy CT reliably identify adrenal adenomas?“ besteht eine geteilte Erstautorenschaft zwischen Herrn Prof. Dr. med. A. Helck und Nicolai Hummel.

Von Herrn Prof. Dr. med. Helck stammt die Fragestellung und somit die Idee zur Studie sowie die initiale Studienplanung und das Studiendesign. Außerdem erfolgte eine kontinuierliche Begleitung bei der Verfassung des Manuskripts durch Verbesserungs- und Ergänzungsvorschläge. Insgesamt erfolgte eine stetige Beratung bei fachlichen Fragen.

Von Herrn Hummel wurde die gesamte Datenerhebung eingebracht.

So wurde beispielsweise die Patientendatenbank des Institut für Klinische Radiologie der LMU (Syngo Imaging / Syngo RIS, Siemens AG Healthcare) anhand spezieller Suchbegriffe durchsucht. Wodurch DECT-Datensätze mit auffälligen Nebennierenbefunden detektiert wurden. Ob diese sich für die Studie eigneten, wurde wie folgt geprüft:

Es wurde nach geeigneten innerklinischen radiologischen follow-up-Untersuchungen (CT, MRT, PET-CT) gesucht und diese ausgewertet. Lagen die benötigten radiologischen Untersuchungen vor, so wurde sichergestellt, dass anhand weiterer Befunde die Dignität der jeweiligen Nebennierenraumforderungen bestimmt werden konnte.

Hierfür wurde die Klinik-Datenbank der Universitätsklinik der LMU unter anderem auf Entlassungsbriefe sowie auf OP-Berichte und histopathologische Befundberichte durchsucht. Ergebnisse hieraus, beispielsweise bezüglich Vorerkrankungen der Patienten oder Dignität des entfernten Tumors wurden erfasst.

Um auch nicht digital verfügbare Unterlagen, wie zum Beispiel externe Arztbriefe oder Dokumentation zur ambulanten Verlaufsuntersuchungen auswerten zu können, wurden die Patientenakten im Archiv des Universitätsklinikum Großhadern gesichtet.

Des Weiteren erfolgte die Bildbearbeitung und Bildauswertung durch Herrn Hummel.

Hierunter fällt die Erstellung der VNC. Diese geschah an der Dual-Energy-Workstation mit der Software Syngo.via “CT Dual Energy“ von Siemens Healthcare. Dort wurde in mehreren Schritten aus den kontrastmittelverstärkten DECT-Bildserien digital das Kontrastmittel entfernt.

Außerdem fallen hierunter Messungen von Größendurchmessern sowie Houndsfield-

Einheiten (HU), jeweils im DECT-Kontrastmittelbild, im DECT-Nativbild sowie im VNC. Ferner erfolgte die Erhebung von Werten, wie z.B. der angefallenen Strahlendosis sowie von Durchschnittswerten und Standardabweichungen.

Es erfolgte zudem die Erfassung technischer Daten bezüglich der durchgeführten DECT-Scans. Insbesondere wurden für jeden Patienten Dosislängenprodukt (DLP) sowie Dosis Index für CT (CTDI) erfasst und hierfür Mittelwerte und Standardabweichungen bestimmt. Diese Daten sind zur Beurteilung der Strahlenbelastung essentiell.

Überdies wurde die initiale statistische Auswertung von Herrn Hummel durchgeführt.

Die erste Fassung des Manuscripts sowie alle Graphiken wurden von Herrn Hummel erstellt und die Manuskripterstellung wurde von ihm bis zur Annahme der finalen Fassung durch European Radiology begleitet.

Die Studie wurde zudem als wissenschaftlicher Vortrag beim ECR 2013 in Wien vorgestellt, welcher von Herrn Hummel erstellt wurde.

Auch die Literaturrecherche wurde überwiegend von Herrn Hummel durchgeführt.

An der zweiten Veröffentlichung, der Studie „Dual energy CT allows for improved characterization of response to antiangiogenic treatment in patients with metastatic renal cell cancer" beteiligte sich Herr Hummel wie im Folgenden beschrieben.

Es erfolgte die Erfassung technischer Daten bezüglich der durchgeführten DECT-Scans. Insbesondere wurden für jeden Patienten Dosislängenprodukt (DLP) sowie Dosis Index für CT (CTDI) erfasst und hierfür Mittelwerte und Standardabweichungen bestimmt. Diese Daten sind zur Beurteilung der Strahlenbelastung essentiell.

Des Weiteren erfolgte die Mitbeurteilung der finalen Fassung des Manuscripts vor Einreichen desselben bei „European Radiology".

4 Zusammenfassung

4.1 Deutsche Fassung

Beide vorgelegten Studien handeln von DECT-spezifischer Bildnachbearbeitung, welche auf der Möglichkeit der quantitativen Iod-Detektion mittels DECT basiert. Diese wurde auf zwei Fragestellungen der onkologischen Radiologie angewandt.

Die Studie „Can single-phase dual-energy CT reliably identify adrenal adenomas“ untersucht die Möglichkeit der Differenzierung von unklaren Nebennierenraumforderungen mittels virtuell generierter Nativbilder (VNC). Hierfür wurden retrospektiv 51 Patienten mit adrenalen Raumforderungen, welche eine kontrastmittelverstärkte DECT (140/100 or 140/80 kVp) erhalten haben, in die Studie eingeschlossen. Aus diesen DECT-Serien wurden VNC erstellt. Zeigten die adrenalen Raumforderungen in den VNC Dichtewerte von ≤ 10 HU, so wurden - analog zu normalen nativen CT-Untersuchungen - adrenale Adenome diagnostiziert. Als Referenzstandard wurden klinisches follow-up, Nativ-CT-Untersuchungen, opposed-phase MRT oder histopathologische Befunde herangezogen. Anhand dieser Referenzstandards wurden 80,7 Prozent als Adenome oder andere benigne Nebennierenläsionen gewertet, neun maligne Raumforderungen wurden erfasst. Bezüglich der Differenzierung zwischen malignen und benignen Läsionen anhand der Dichtewertschwelle von 10 HU im VNC betrug die Sensitivität der Methode 73 %, die Spezifität 100%, die Genauigkeit 81%. Die Studie zeigt somit, dass aus kontrastmittelverstärkten DECT-Serien generierte virtuelle Nativbilder zur korrekten Diagnosestellung bei fettreichen adrenalen Raumforderungen herangezogen werden können und dass sie somit helfen können, zusätzliche Untersuchungen zu vermeiden.

In der Studie „Dual energy CT allows for improved characterization of response to antiangiogenic treatment in patients with metastatic renal cell cancer “ wurde die Rolle der DECT-Technologie in der Beurteilung von antiangiogenetischen Effekten von Antikörper-Therapie bei Nierenzellkarzinomen (NZK) untersucht.

Bei 26 Patienten mit NCC wurden vor Beginn der Therapie mit Tyrosinkinaseinhibitoren (TKI) sowie 10 Wochen danach kontrastmittelverstärkte DECT-Untersuchungen durchgeführt. Aus diesen DECT-Serien wurden farbkodierte

Iod-Bildserien generiert. Die Iod-Dichte (ID) sowie der Iod-Gehalt (IC) in mg/ml des Gewebes wurden bestimmt. Die auf diese Weise generierten Werte wurden mit Werten der venösen Phase der Kontrastmittel-DECT (CTD) verglichen. Im Vergleich zwischen Ausgangs- und Verlaufsuntersuchung zeigten sowohl CTD als auch ID eine signifikante Reduktion der Iod-Aufnahme der NCC-Metastasen nach TKI-Therapie. Allerdings war die relative Reduktion der Iod-Aufnahme für ID signifikant größer als für CTD. Die Studie zeigte, dass mittels DECT-Datensätzen eine Quantifizierung der Iod-Aufnahme von NCC-Metastasen möglich ist. Ferner konnte gezeigt werden, dass antiangiogene TKI-Therapieeffekte mit signifikant besserer Sensitivität und Reproduzierbarkeit erkannt werden können als mit der normalen CTD.

4.2 Englische Fassung

Both studies deal with diagnostic tools which enable dual energy CT-based iodine quantification. These tools were applied in two different clinical scenarios in oncologic patients.

The study „Can single-phase dual-energy CT reliably identify adrenal adenomas“ evaluates whether attenuation measurements on virtual non contrast images (VNC) can reliably differentiate adrenal incidentaloma.

51 patients with adrenal masses who had undergone contrast-enhanced dual-energy-CT (140/100 or 140/80 kVp) were retrospectively identified. Virtual non contrast images were generated. Adrenal adenoma was diagnosed if density on virtual non-contrast images was ≤10 HU. Clinical follow-up, true non-contrast CT, PET/CT, in- and opposed-phase MRI, and histopathology served as the standard of reference. Based on the standard of reference, 80.7 % adrenal masses were characterised as adenomas or other benign lesions; 9 malignant lesions were detected. Based on the threshold of 10 HU on the virtual non-contrast images, the sensitivity, specificity, and accuracy for the differentiation of benign and malingant adrenal lesions was 73 %, 100 %, and 81 % respectively. VNC images derived from dualenergy- CT allow for accurate characterisation of lipid-rich adrenal adenomas and can help to avoid additional follow-up imaging.

The study „Dual energy CT allows for improved characterization of response to antiangiogenic treatment in patients with metastatic renal cell cancer “ evaluated the value of dual energy CT (DECT) in detecting antiangiogenic treatment effects of tyrosine kinase inhibitors (TKI) in patients with metastatic renal cell cancer (mRCC).

26 patients with mRCC were examined with abdominal contrast enhanced DECT-scans before start of TKI-therapy and 10 weeks later. Colour-coded iodine images were generated. Additionally, iodine density (ID) and tissue iodine content (IC) in mg/ml were calculated. ID and IC were compared to the venous phase DECT density (CTD) of the lesions. Both CTD and ID of RCC metastases decreased significantly between baseline and follow up. However, relative reduction of Iodine uptake was significant greater for ID than for CTD. The study showed that quantification of iodine content of mRCC-metastasis is possible. In addition it was shown that antiangiogenic treatment effects of TKI can be detected at a significantly highersensitivity and reproducibility.

5 Veröffentlichung I

A. Helck, N. Hummel (contributed equally) et. al.: „Can single-phase dual-energy CT reliably identify adrenal adenomas?", European Radiology, Juli 2014.
Siehe Anhang.

Die originale Publikation ist auf www.springerlink.com verfügbar.
(https://link.springer.com/article/10.1007%2Fs00330-014-3192-z)

6 Veröffentlichung II

K. Hellbach, N. Hummel et. al.: „Dual energy CT allows for improved characterization of response to antiangiogenic treatment in patients with metastatic renal cell cancer ", European Radiology, September 2016.
Siehe Anhang.

Die originale Publikation ist auf www.springerlink.com verfügbar.
(https://link.springer.com/article/10.1007%2Fs00330-016-4597-7)

7 Literaturverzeichnis

1. BAfS. "Röntgendiagnostik: Häufigkeit und Strahlenexposition". Bundesamt für Strahlenschutz. 2016.

2. Sedlmair M. "Dual-Energy CT: Physikalische Modelle und Anwendungen.", Dissertation, LMU München: Medizinische Fakultät. 2009.

3. Coursey CA, Nelson RC, Boll DT, Paulson EK, Ho LM, Neville AM, et al. Dual-energy multidetector CT: how does it work, what can it tell us, and when can we

use it in abdominopelvic imaging? Radiographics : a review publication of the Radiological Society of North America, Inc. 2010 Jul-Aug;30(4):1037-55. PubMed PMID: 20631367.

8 Danksagung

Zuallererst bedanke ich mich bei meiner Ehefrau, ohne deren geduldige Unterstützung die Erstellung dieser Arbeit undenkbar gewesen wäre.

Mein besonderer Dank gilt Herrn Prof. Dr. med. Andreas Dietrich Helck für die kompetente und persönliche Betreuung, die aufgebrachte Geduld sowie die wiederholte Motivation über die gesamte Dauer der Erstellung der vorliegenden Arbeit. Ferner auch für die Einführung in das Schreiben wissenschaftlicher Artikel.

Herzlich bedanken möchte ich mich bei Herrn Prof. Dr. med. Anno Graser für die Einführung in die Dual-Energy-post-processing Software und die freundliche Beratung und Unterstützung bei der Erstellung meiner ersten Studie.

Des Weiteren bedanke ich mich sehr herzlich bei Frau Dr. med. Katharina Hellbach für die Möglichkeit, meine im Rahmen der ersten Arbeit erworbenen Kenntnisse in ihre Studie einzubringen sowie für die freundliche und konstruktive Zusammenarbeit.

Im übrigen Danke ich den allen Mitarbeitern des Instituts für Klinische Radiologie, welche mir bei Software-Problemen wiederholt helfen konnten.

9 Anhang

Im Anhang finden sich die beiden Veröffentlichungen (siehe Kapitel 5 sowie Kapitel 6), welche im Rahmen der kumulativen Dissertation vorgelegt werden.

Can single-phase dual-energy CT reliably identify adrenal adenomas?

A. Helck • N. Hummel • F. G. Meinel • T. Johnson • K. Nikolaou • A. Graser

Received: 13 December 2013 /Revised: 10 March 2014 /Accepted: 15 April 2014 # European Society of Radiology 2014

Abstract

Purpose

To evaluate whether single-phase dual-energy-CTbased attenuation measurements can reliably differentiate lipid-rich adrenal adenomas from malignant adrenal lesions.

Materials and methods

We retrospectively identified 51 patients with adrenal masses who had undergone contrastenhanced dual-energy-CT (140/100 or 140/80 kVp). Virtual non-contrast and colour-coded iodine images were generated, allowing for measurement of pre- and post-contrast density on a single-phase acquisition. Adrenal adenoma was diagnosed if density on virtual non-contrast images was ≤10 HU. Clinical follow-up, true non-contrast CT, PET/CT, in- and opposed-phase MRI, and histopathology served as the standard of reference.

Results

Based on the standard of reference, 46/57 (80.7 %) adrenal masses were characterised as adenomas or other benign lesions; 9 malignant lesions were detected. Based on a cutoff value of 10 HU, virtual non-contrast images allowed for correct identification of adrenal adenomas in 33 of 46 (71 %), whereas 13/46 (28 %) adrenal adenomas were lipid poor with a density ≥10 HU.

A. Helck and N. Hummel contributed equally to this work.

A. Helck • N. Hummel • F. G. Meinel • T. Johnson • K. Nikolaou • A. Graser

Institute for Clinical Radiology, University of Munich, Grosshadern
Campus, Marchioninistr. 15, 81377 Munich, Germany
e-mail: andreas.helck@med.uni-muenchen.de

Based on the threshold of 10 HU on the virtual non-contrast images, the sensitivity, specificity, and accuracy for detection of benign adrenal lesions was 73 %, 100 %, and 81 % respectively. Conclusion Virtual non-contrast images derived from dualenergy-CT allow for accurate characterisation of lipid-rich adrenal adenomas and can help to avoid additional follow-up imaging.

Key Points *• Adrenal adenomas are a common lesion of the adrenal glands. • Differentiation of benign adrenal adenomas from malignant adrenal lesions is important. • Dual-energy based virtual non-contrast images help to evaluate patients with adrenal adenomas*.

Keywords Dual-energy CT . Virtual non-contrast images . Adrenal lesion . Adrenal adenoma . Reduction of dose exposure

Introduction

Adrenal masses are common pathologies with an incidence between 4.4 % and 9.0 % [1–5] on abdominal CTs. Since cross-sectional abdominal imaging is increasingly used, incidental adrenal masses are discovered more frequently. The majority of adrenal masses are benign adenomas. However, several malignant tumours metastasise to the adrenal glands and up to 2.5 % of adrenal incidentalomas turn out to be metastases [6, 7]. Hence, the differentiation between benign and malignant adrenal masses is of great importance, especially in patients with known malignancy. In principle, the diagnosis of a benign adenoma can easily be established by detection of intracellular fat on non-contrast CT images as about 70 % of adrenal adenomas contain a large amount of intracellular fat (mainly cholesterol and fatty acids) [8]. The diagnosis of this sort of adenoma can be assumed with a sensitivity of 70 % and specificity of 98 % when measurements show Hounsfield numbers lower than 10 on non-contrast CT. This has been proven by various studies showing that lipid-rich adenomas can be accurately differentiated from malignant lesions on non-contrast CT images because of their low density [9–11].

However, in clinical routine, few abdominal CT examinations include a non-contrast acquisition, and contrast enhancement frequently masks fatty contents in lipid-rich adenomas,

thereby making density measurements unreliable. In this setting, further imaging is required for accurate characterisation of unclear adrenal masses: either a non-contrast CT examination or a delayed phase examination showing fast washout of contrast agent has to be performed [6]. However, both procedures are time consuming and cause additional radiation exposure. Another option for adrenal mass characterisation is MRI chemical shift imaging using an in and opposed phase [8, 12]. This type of additional imaging is time consuming and associated with significant additional costs. An ideal solution for this dilemma is dual-energy CT. The technology has shown great potential in numerous clinical indications in the abdomen [13]. Since it enables subtraction of iodine from a contrast-enhanced CT examination by means of three material decomposition techniques, it provides the same diagnostic information as a biphasic CT examination containing a noncontrast and a contrast-enhanced phase [14, 15]. This information could be used to characterise unclear adrenal masses on a single-phase examination [12, 16]. The purpose of this study was to assess the accuracy of DECT in the differentiation of lipid-rich adrenal adenomas from malignant adrenal masses using single-phase dual-energy contrast-enhanced abdominal CT.

Materials and methods

Patient population

Our in-house patient database (Syngo Imaging/Syngo RIS, Siemens AG Healthcare, Forchheim, Germany) was accessed using specific search terms ("dual energy" AND “adrenal”~OR “adrenal adenoma”~OR “adrenal lesion”~OR “incidentaloma”~OR “adrenal metastasis”) in order to identify patients who (1) had undergone abdominal DECT and (2) had reported abnormalities of the adrenal glands. Thus, we retrospectively identified all patients with adrenal masses of at least 1 cm who had undergone single-phase contrast-enhanced DECT examinations of the abdomen and included these individuals in the study. IRB approval was waived.

CT protocol

CT imaging was performed on one of two dual-source multidetector row CT systems (Somatom Definition Dual Source, n=x or Somatom Definition Flash, n=y; Siemens Healthcare,

Forchheim, Germany). Each of these systems consists of two X-ray tubes and their corresponding detectors mounted in an approximately 90-degree angle. Patients were positioned on the CT table in the supine position. The Somatom Definition (first-generation system) had a field of view of 26 cm (FOV) on its smaller detector (26 cm), whereas the Somatom Definition Flash (second-generation system) provides a FOV of 33 cm on the smaller detector. The larger detectors have an identical size and cover 50 cm; 70 s after intravenous injection of a nonionic contrast agent (1.35 ml/kg patient body weight; Ultravist 370, BayerSchering Diagnostics, Berlin, Germany), a dual-energy examination of the abdomen was acquired operating the “A” tube at 140 kVp (140 kVp with tin filtering, Sn140 kVp for the Flash CT) and the “B” tube at 80 kVp (100 kVp for the Flash CT). For both tubes, an automated attenuation-based tube current modulation (CareDOSE 4D, Siemens, Forchheim, Germany) was used. All examinations were acquired at a pitch of 0.55 to 0.6; the gantry rotation speed was 0.5 s [17, 18]. The dose length products (DLPs) were recorded from the patient protocol and were used for calculation of estimates of individual effective radiation doses in mSv using an organ-based standard conversion factor for abdominal CT (0.015 mSv/mGy*cm).

Dual-energy post processing and image reconstruction

From one DECT examination, three different sets of images are created: one low- and one high-kVp data set, and weighted average images, which are based on data from both detectors, using 70 % information from the high kV and 30 % from the low kV examination (Definition DS) and 50 % from each kV examination (Definition Flash). These images resemble image quality of a standard 120-kVp CT examination. For post processing, a dedicated dual-energy workstation (syngo Multi-Modality Workplace, Somaris Version CT2008G; Siemens Healthcare) was used. An application called “Liver VNC” was utilised to create images from which iodine had been subtracted [15, 17]. This calculation is based on a so-called three-material decomposition analysis [19]. The 3-mm-thick virtual noncontrast images were reconstructed from the raw data using a 2-mm reconstruction

increment to allow for exact three-material decompositions at limited image noise.

Analysis of adrenal lesions

For assessment of lesion size, a volumetric analysis using the “volume” software (syngo MMWP, Siemens Healthcare, Erlangen/Germany) of each adrenal lesion was performed. The density of all adrenal lesions was measured on both contrast-enhanced and virtual non-contrast images. The mean HU was calculated by performing three repetitive measurements; the respective ROI was placed centrally in the lesion and was adapted to lesion size to avoid a partial volume effect.

Characterisation of adrenal masses as benign or malignant

For the assessment of lesion aetiology clinical follow-up (n=12), true non-contrast CT (n=26), PET/CT (n=5), inand opposed-phase MRI (n=5), and histopathology (n=9) were used. A benign lesion was diagnosed when there was lack of size progression for at least 6 months. In ten patients without medical history of malignancy, no follow-up imaging was performed. In these cases a clinical follow-up of at least 18 months was considered diagnostic for absence of malignancy [3, 8, 20, 21].

Statistical analysis

Sensitivity, specificity, and accuracy of dual-energy virtual non-contrast images for the characterisation of incidental adrenal masses were calculated using chi-square tables of contingency.

Results

In the study period, n=457 abdominal dual-energy CT examinations were performed at our department. In 51 of these patients, adrenal incidentalomas were detected and these individuals formed the study population. DECT examinations were performed between April 2007 and September 2012. The patient population consisted of 28 men and 23 women (mean age, 70±13 years; range, 24−85 years); 53 % of patients (n=27) had adrenal masses on the left side, 35 % (n=18) on the right, and in 12 % (n=6) both sides were affected. In total, 57 adrenal masses were identified. Tables 1 and 2 describe patient characteristics in detail and gives more information about the final diagnosis.

Based on the reference standard, 48 adrenal masses turned out to be benign lesions and in 9 patients malignant lesions were diagnosed. All lesions with HU >10 HU (n=35 or 73% of benign lesions) on virtual non-contrast images proved to be bening, whereas 27 % (n=13) of the benign masses showed densities of ≥10 HU on virtual non-contrast images. All malignant lesions (n=9) showed a density of ≥10 HU on virtual non-contrast images.

Figure 1 illustrates the status (benign versus malignant) of the adrenal lesions with respect to HU values. Table 3 shows the maximum diameter and volume of the adrenal lesions respectively.

The majority of benign lesions were adrenal adenomas (n=46), of which 72 % were lipid-rich (mean density of -1.3 ±8.7 HU, range: -22.5–9.6) and 28 % were lipid-poor adenomas (mean density of 21.2±11.1 HU, range 10.3–41.0). The remaining two benign lesions, both of which were easily diagnosed by dual-energy CT based on their characteristic imaging appearance, were one lipoma (-67.4 HU) and one myelolipoma (-67.1 HU). The mean density value of the nine malignant adrenal masses was 25.3±11.1 HU (range 11.0– 48.1 HU). Figure 2 shows the DECT examination of a lipid-rich adenoma of the left adrenal gland with normal enhancement masking the lipid content in the contrastenhanced images. An adrenal metastasis of renal cell carcinoma is shown in Figure 3.

Based on the threshold of 10 HU on the virtual noncontrast images, the sensitivity, specificity, and accuracy for detection of lipid-rich adrenal adenomas in our study were 71 %, 81 %, and 74 % respectively. The sensitivity, specificity, and accuracy for differentiation of benign versus malignant adrenal lesions were 73 %, 100 %, and 81 % respectively. Mean estimated radiation exposure by contrast-enhanced single-phase DECT examinations of the abdomen was 7.9± 3.9 mSv (3.3 to 14.7 mSv).

Discussion

In clinical routine, incidentally detected adrenal nodules that enhance with contrast require further workup, as portal venous phase CT is unable to discriminate benign from malignant lesions. Since this is most often connected with additional dose exposure as well as cost, we sought to

evaluate the potential of DECT in the characterisation of adrenal masses and to differentiate them from malignant lesions.

Gupta et al. first used DECT for characterisation of adrenal lesions by evaluating the attenuation difference of adrenal lesions on high- and low-kVp non-contrast DECT images. Although a decrease in attenuation (0.4±7.1 HU for adenomas and 9.2±4.3 HU for metastatic lesions) was highly specific (100 %) for diagnosis of an adrenal adenoma, the sensitivity was relatively low (50 %) [16]. In contrast to these results, we used virtual non-contrast CT images (calculated from contrast-enhanced DECT examinations) and a cutoff value of 10 HU to differentiate benign from malignant adrenal masses. Regarding characterisation of adrenal adenomas, we observed better results with sensitivity, specificity, and accuracy in our patient population of 71 %, 81 %, and 74 % respectively. Regarding differentiation of benign versus malignant lesions, virtual non-contrast DECT images allowed for superior sensitivity and accuracy of 73 % and 81 %, whereas the same level of specificity was achieved (100 %). Thus, in theory, no further imaging is required in about two-thirds of patients with incidentalomas.

The study of Gnannt et al. [12] and Ho et al. [22] showed that DECT-based virtual non-contrast images are comparable to true non-contrast CT images and therefore principally allow for the characterisation of adrenal incidentalomas. However, because of the relative small number of reported cases, in our opinion further evidence is needed to support the use of this new technique as a diagnostic tool. In contrast to the aforementioned studies we furthermore used a slightly different study design and did not routinely acquire an additional true non-contrast examination, which helped to avoid additional dose exposure to the study population. Instead, in half of the cases we correlated the results of the virtual non-contrast images with clinical follow-up, PET/CT, in- and opposedphase MRI, and histopathology respectively. Therefore our study design seems to be more consistent with routine clinical practice, too.

Gnannt et al. [12] achieved a sensitivity, specificity and accuracy of nearly 100 % (95/100/97) for lipid-rich adrenal adenomas when matching virtual non-contrast DECT images with true non-contrast images. It is well known that the quality of virtual non-

contrast images is slightly lower compared to true non-contrast images [23], and Kim et al. [24] observed aberrations regarding attenuation values in the virtual noncontrast images, which can be especially troublesome when dealing with small structures. However, our results do not indicate reduced sensitivity of virtual non-contrast images, since the sensitivity of 71 % for detection of lipid rich adenomas is in accordance with the sensitivity of true unenhanced CT examinations [8, 11]. Furthermore, increased image noise and differences of attenuation values primarily occurred with first-generation DECT [15] and quality of virtual non-contrast images substantially improved with second-generation DECT [25, 26]. Thus, it is now widely accepted that in abdominal imaging, virtual non-contrast images can replace true unenhanced examinations at least in normal-size patients, thereby helping to reduce radiation exposure to the patient by eliminating true non-contrast acquisitions [26]. The amount of dose reduction depends on respective tube settings of the true unenhanced examination and values of 19 to 41 % have been described [12, 15, 7]. One potential disadvantage of single-phase contrast-enhanced DECT examinations is the slightly elevated dose exposure of approximately 8 % compared to a contrast-enhanced single-energy examination at 120 kVp [6]. Yet, given the numerous advantages of DECT, its application in abdominal imaging seems highly beneficial.

Our study has several limitations. It was conducted in a retrospective fashion causing potential selection bias with regard to the study population. However, our patient collective represents the distribution to be expected in an active oncological service. Furthermore, we did not acquire true noncontrast CT examinations to compare with our virtual noncontrast images. However, the diagnostic quality and potential of DECT-based virtual non-contrast images have been demonstrated in various clinical trials [13]; at our department, several abdominal CT protocols that require non-contrast examinations are routinely performed on the dual-source CT without a non-contrast phase. Moreover, the diagnosis of adrenal adenomas in our study was not confirmed by histopathology in all cases, but by an imaging-based reference standard or long-term clinical follow-up. As adrenal

nodules characterised as benign on cross-sectional imaging will not be removed, this limitation cannot be easily overcome. Biopsies would not have been ethically justified in this setting and an imaging-based approach has been widely accepted [21]. Finally, the proposed DECT protocol does not enable differentiation between lipid-poor adenomas and malignant adrenal masses. In this patient population, additional delayed-phase imaging is required for calculation of the washout rate and characterisation of lesions [16].

Conclusion

The results of the present study indicate that virtual noncontrast images can be used to reliably differentiate lipidrich adenomas and malignant adrenal lesions. In patients with adrenal nodules detected incidentally on abdominal contrastenhanced CT, this method has great potential to reduce costly follow-up imaging and associated radiation exposure to the patient.

Acknowledgements The scientific guarantor of this publication is Prof. Dr. Anno Graser. The authors of this manuscript declare no relationships with any companies, whose products or services may be related to the subject matter of the article. The authors state that this work has not received any funding. No complex statistical methods were necessary for this paper. Institutional Review Board approval was obtained. Written informed consent was waived by the Institutional Review Board. Methodology: retrospective, diagnostic or prognostic study, performed at one institution

Tables and Figures

TABLE 1. Scan Parameters for the 2 Dual Source Scanners

	Definition DS (Tubes A/B)	**Definition Flash (Tubes A/B)**
Slices	2 x 64	2 x 128
Angular offset (°)	90	95
FoV (cm)	50/26	50/33
Spectra (kVp)	140/80	100/Sn140
Filter (mm)	3 A1, 0.9 Ti	3 A1, 0.9, Ti, 0.4 Sn (B tube only)
Current time product (mAs)	96/404	300/232
Modulation	CareDose4D (x, y, z-axis)	CareDose 4D (x, y, z-axis)
Collimation (mm)	14 x 1.2	32 x 0.6
Pitch	0.55	0.6
Rotation time (s)	0.5	0.5

Definition DS indicates first generation dual source CT; Definition FLASH, second generation dual source CT.

TABLE 2. Patient characteristics with underlying disease and final diagnoses

n	Underlying disease	Adenoma (n=45)	other adrenal lesions (n=3)	Metastasis (n=8)
	malignant			
10	Renal Cell carcinoma	7	-	3
5	GIST	5	-	-
4	Pancreatic ductal adenocarcinoma	2	-	2
3	Colon carcinoma	3	-	-
2	Oropharyngeal squamous cell carcinoma	1	-	1
1	Acute lymphocytic leukaemia	-	-	1
1	Adenocarcinoma of the lung	1	-	-
1	Chondrosarcoma	1	-	-
1	Gastric adenocarcinoma	-	-	1
1	Invasive ductal carcinoma	1	-	-
1	Ovarian carcinoma	1	-	-
1	Pheochromocytoma	-	Pheochromocytoma	-
1	Seminoma	1	-	-
	benign			
6	Abdominal aortic aneurysm	5	Lipoangioma	-
4	Unknown lesion of the renal bed	4	-	-
2	Coronary heart disease	2	-	-
2	Hormonactive adrenal adenoma	2	-	-
2	Lumbago	2	-	-
1	Anemia of unknown origin	1	-	-
1	Arterial hypertension	1	-	-
1	Atrial septal defect	1	-	-
1	Barrett's esophagus	1	-	-
1	Benign prostatic hyperplasia	1	-	-
1	Heart transplantation	-	Myelolipoma	-
1	Peripheral arterial occlusive disease	1	-	-
1	Pulmonary embolism	1	-	-
1	Unknown lymphadenopathy	1	-	-

TABLE 3. Maximum diameter and volume of adrenal lesions

	Adenoma < 10 HU	Adenoma > 10 HU	Metastasis	Total*
Maximum Diameter				
Average (mm)	27.1	28.5	32.1	29.2
Standard deviation (mm)	8.5	15.5	7.2	12.6
Minimum (mm)	13.7	16.4	16.3	13.7
Maximum (mm)	37.4	75.3	38.0	83.9*
Volumetry				
Average (ml)	6.7	17.8	9.5	13.7
Standard deviation (ml)	5.0	42.8	9.1	32.6
Minimum (ml)	1.2	1.5	2.9	1.2
Maximum (ml)	14.2	160.0	34.8	182.1*

* This column includes the adrenal myelolipoma, which was the largest adrenal mass measured in this study.

FIGURE 1. Status (benign versus malignant) of the adrenal lesions with respect to HU values

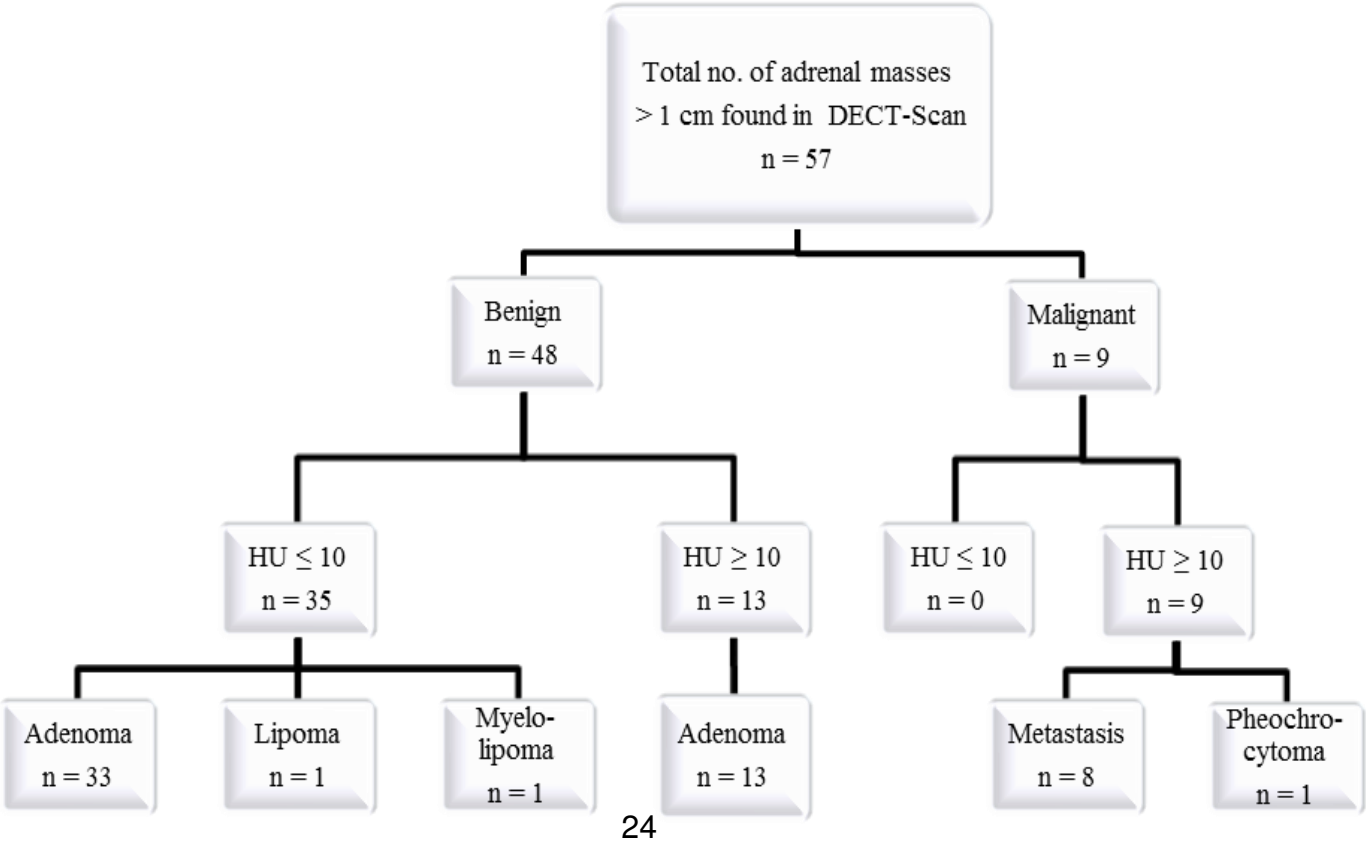

FIGURE 2. Contrast enhanced DE-CT of the abdomen in the portal venous phase: 2 cm large lesion of the left adrenal gland with density of 48 HU (A). Virtual non-contrast image (B) shows a density HU < 10. CM-enhancement is shown in the iodine overlay images (C). In- and opposed phase MRI confirmed diagnosis of a lipid rich adenoma.

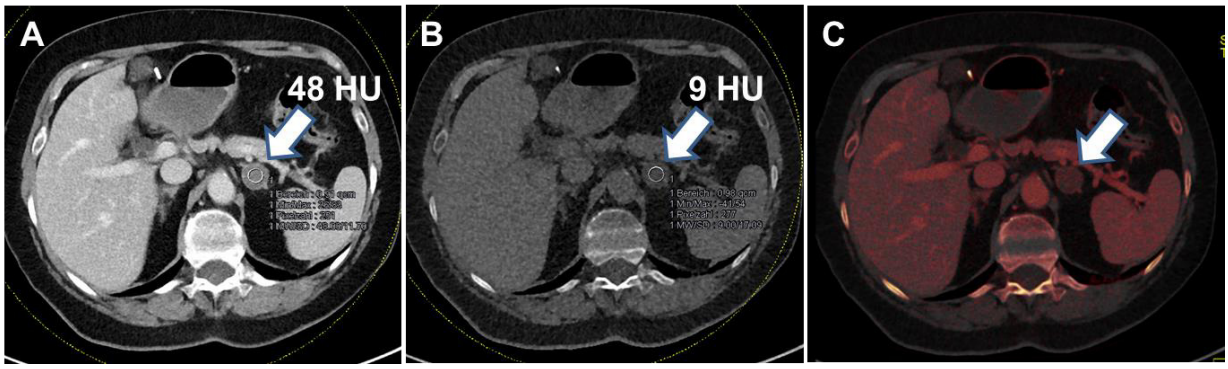

FIGURE 3. Contrast enhanced DE-CT of the abdomen in the portal venous phase: 2,7 cm large lesion of the left adrenal gland with density of 36 HU (A). Virtual non-contrast image (B) shows a density of 21 HU. CM-enhancement is shown in the iodine overlay images (C). Metastasis of a renal cell carcinoma in the left adrenal gland.

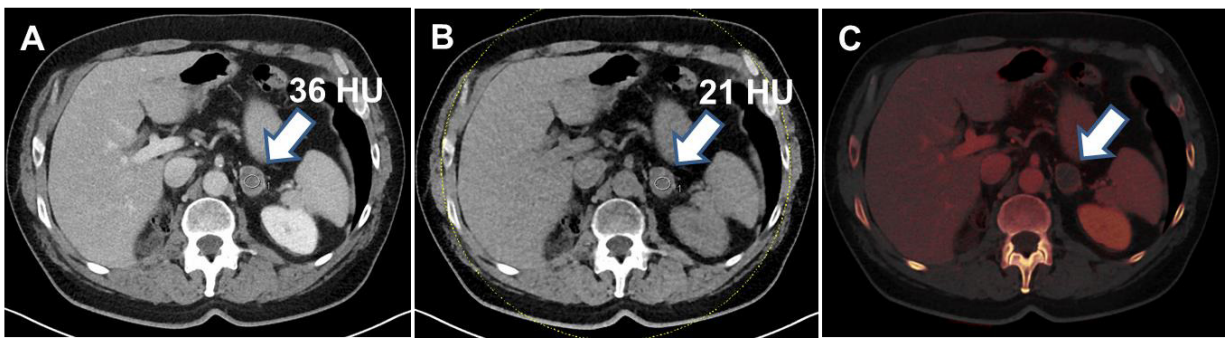

References

1. Bovio S, Cataldi A, Reimondo G et al (2006) Prevalence of adrenal incidentaloma in a contemporary computerized tomography series. J Endocrinol Invest 29:298–302
2. Song JH, Chaudhry FS, Mayo-Smith WW (2008) The incidental adrenal mass on CT: prevalence of adrenal disease in 1,049 consecutive adrenal masses in patients with no known malignancy. AJR Am J Roentgenol 190:1163–1168
3. Dunnick NR, Korobkin M (2002) Imaging of adrenal incidentalomas: current status. AJR Am J Roentgenol 179:559–568
4. Dunnick NR, Korobkin M, Francis I (1996) Adrenal radiology: distinguishing benign from malignant adrenal masses. AJR Am J Roentgenol 167:861–867
5. Young WF Jr (2007) Clinical practice. The incidentally discovered adrenal mass. N Engl J Med 356:601–610
6. Lam KY, Lo CY (2002) Metastatic tumours of the adrenal glands: a 30-year experience in a teaching hospital. Clin Endocrinol (Oxf) 56: 95–101
7. Young WF Jr (2000) Management approaches to adrenal incidentalomas. A view from Rochester, Minnesota. Endocrinol Metab Clin North Am 29:159–185, x
8. Blake MA, Cronin CG, Boland GW (2010) Adrenal imaging. AJR Am J Roentgenol 194:1450–1460
9. Yip L, Tublin ME, Falcone JA et al (2010) The adrenal mass: correlation of histopathology with imaging. Ann Surg Oncol 17: 846–852
10. Legmann P (2009) Adrenal incidentaloma: management approaches: CT - MRI. J Radiol 90:426–443 Eur Radiol
11. Boland GW, Lee MJ, Gazelle GS et al (1998) Characterization of adrenal masses using unenhanced CT: an analysis of the CT literature. AJR Am J Roentgenol 171:201–204
12. Gnannt R, Fischer M, Goetti R et al (2012) Dual-energy CT for characterization of the incidental adrenal mass: preliminary

observations. AJR Am J Roentgenol 198:138–144

13. Heye T, Nelson RC, Ho LM et al (2012) Dual-energy CTapplications in the abdomen. AJR Am J Roentgenol 199:S64–70
14. Brown CL, Hartman RP, Dzyubak OP et al (2009) Dual-energy CT iodine overlay technique for characterization of renal masses as cyst or solid: a phantom feasibility study. Eur Radiol 19:1289–1295
15. De Cecco CN, Buffa V, Fedeli S et al (2010) Dual energy CT (DECT) of the liver: conventional versus virtual unenhanced images. Eur Radiol 20:2870–2875
16. Gupta RT, Ho LM, Marin D et al (2010) Dual-energy CT for characterization of adrenal nodules: initial experience. AJR Am J Roentgenol 194:1479–1483
17. Graser A, Johnson TR, Hecht EM et al (2009) Dual-energy CT in patients suspected of having renal masses: can virtual nonenhanced images replace true nonenhanced images? Radiology 252:433–440
18. Flohr TG, McCollough CH, Bruder H et al (2006) First performance evaluation of a dual-source CT (DSCT) system. Eur Radiol 16:256–268
19. Liu X, Yu L, Primak AN et al (2009) Quantitative imaging of element composition and mass fraction using dual-energy CT: three-material decomposition. Med Phys 36:1602–1609
20. Mayo-Smith WW, Boland GW, Noto RB et al (2001) State-of-the-art adrenal imaging. Radiographics 21:995–1012
21. Boland GW, Blake MA, Hahn PF et al (2008) Incidental adrenal lesions: principles, techniques, and algorithms for imaging characterization. Radiology 249:756–775
22. Ho LM, Marin D, Neville AM et al (2012) Characterization of adrenal nodules with dual-energy CT: can virtual unenhanced attenuation values replace true unenhanced attenuation values? AJR Am J Roentgenol 198:840–845
23. Zhang LJ, Peng J, Wu SYet al (2010) Liver virtual non-enhanced CT with dual-source, dual-energy CT: a preliminary

study. Eur Radiol 20:2257–2264
24. Kim YK, Park BK, Kim CK et al (2013) Adenoma characterization: adrenal protocol with dual-energy CT. Radiology 267:155–163
25. Toepker M, Moritz T, Krauss B et al (2012) Virtual non-contrast in second-generation, dual-energy computed tomography: reliability of attenuation values. Eur J Radiol 81:e398–405
26. Graser A, Becker CR, Staehler M et al (2010) Single-phase dualenergy CT allows for characterization of renal masses as benign or malignant. Invest Radiol 45:399–405

Dual energy CT allows for improved characterization of response to antiangiogenic treatment in patients with metastatic renal cell cancer

K. Hellbach • A. Sterzik • W. Sommer • M. Karpitschka • N. Hummel • J. Casuscelli • M. Ingrisch • M. Schlemmer • A. Graser • Michael Staehler

Received: 26 October 2015 /Revised: 31 August 2016 /Accepted: 5 September 2016 #

Abstract

Objectives

To evaluate the potential role of dual energy CT (DECT) to visualize antiangiogenic treatment effects in patients with metastatic renal cell cancer (mRCC) while treated with tyrosine-kinase inhibitors (TKI).

Methods

26 patients with mRCC underwent baseline and follow-up single-phase abdominal contrast enhanced DECT scans. Scans were performed immediately before and 10 weeks after start of treatment with TKI. Virtual non-enhanced (VNE) and color coded iodine images were generated. 44 metastases were measured at the two timepoints. Hounsfield unit (HU) values for VNE and iodine density (ID) as well as iodine content (IC) in mg/ml of tissue were derived. These values were compared to the venous phase DECT density (CTD) of the lesions.

Values before and after treatment were compared using a paired Student's *t* test.

Results

Between baseline and follow up, mean CTD and DECT-derived ID both showed a significant reduction ($p<0.005$). The relative reduction measured in percent was significantly

greater for ID than for CTD (49.8 ± 36,3 % vs. 29.5 ± 20.8 %, p<0.005). IC was also significantly reduced under antiangiogenic treatment (p<0.0001).

Conclusions

Dual energy CT-based quantification of iodine content of mRCC metastases allows for significantly more sensitive and reproducible detection of antiangiogenic treatment effects.

Key points

- A sign of tumor response to antiangiogenic treatment is reduced tumor perfusion.
- DECT allows visualizing iodine uptake, which serves as a marker for vascularization.
- More sensitive detection of antiangiogenic treatment effects in mRCC is possible.

Keywords Metastatic renal cell carcinoma; therapy monitoring; response evaluation; antiangiogenic treatment; dual energy computed tomography

Abbreviations and acronyms

BL	baseline
CTD	dual energy CT density (venous phase)
DECT	dual energy computed tomography
DLP	dose-length product
FU	follow up
GIST	gastrointestinal stromal tumors
HU	Hounsfield unit
IC	iodine concentration
ID	iodine density
IRA	iodine related attenuation
(m)RCC	(metastatic) renal cell cancer
ROI	region of interest
TKI	tyrosine-kinase inhibitor
VEGF	vascular endothelial growth factor
VNE	virtual non-enhanced

Corresponding author: Michael Staehler, MD, PhD
michael.staehler@med.uni-muenchen.de

The other authors are members of the
Department of Clinical Radiology respectively
Department of Urology, both Ludwig-Maximilians-University Hospital Munich, Marchioninistr. 15, 81377 München, Germany
and
Department of Palliative Care, Krankenhaus Barmherzige Brüder München, Romanstr. 93, 80639 München, Germany

Introduction

Renal cell carcinoma (RCC) is the most common form of malignant kidney neoplasm. 25-30% of RCC patients already have metastases at the time of initial diagnosis [1] and 20-40% will develop metachronous metastases after surgery for localized disease [2, 3]. In metastatic RCC (mRCC), systemic therapy based on inhibition of angiogenesis is the treatment standard [4]. Tyrosine- and multi-kinase inhibitors (TKI) are promising therapeutic agents in the treatment of these highly vascularized tumors and their metastases [4, 5]. By down regulation of vascular endothelial growth factor (VEFG) and several other cellular mechanisms they decrease tumor vascularization and blood supply. On standard venous phase CT imaging, therapy-induced changes in lesion size as described by RECIST criteria [6] may be absent or significantly delayed.

Computed tomography (CT) is most commonly used for initial staging and treatment surveillance in mRCC patients [7]. Obviously, response to targeted therapy does not necessarily correlate to change in tumor size. In fact, a decrease in measured tumor CT density, representative of a reduction in the number of tumor vessels, or decreasing enhancement of intratumoral nodules can occur independently from a change in tumor size. Recent studies have shown that besides tumor diameter as a marker of tumor growth, measuring the contrast enhancement in highly perfused tumorous lesions such as RCC might be a more relevant tool to provide information about response to antiangiogenetic treatment [8, 9].

Dual energy CT (DECT) is a relatively new CT technique that allows for the identification and visualization of different materials in the scan field, thereby providing information that goes beyond CT density measurements. Namely, it enables differentiation of iodine from other substances; a useful tool for the assessment of enhancement within complex soft tissue masses. Based on DECT data, it is possible to create iodine maps showing pure iodine-related density (ID), which represents the fraction of the total measured density that is caused by iodine. This parameter therefore yields information about absolute contrast media uptake without taking into account the confounding underlying tissue density, which can be

viewed and quantified separately in a so-called virtual non-contrast image (VNC). A contrast-enhanced venous dual energy CT image combines information from both the ID and VNC image [10, 11].

DECT is of special interest in response imaging of highly perfused tumors [12]. ID images rather than standard contrast-enhanced CT images give information about a lesion's capability to take up contrast media, which is strongly dependent on tumor vascularization. As shown for gastrointestinal stromal tumors (GIST) [13, 14], another highly vascularized tumor entity, ID information correlates better with response to antiangiogenic treatment than tumor size or Choi criteria and therefore might be an independent surrogate biomarker for response to treatment with TKI.

The aim of this study was to investigate whether single-phase DECT allows for improved assessment of response to antiangiogenetic treatment with tyrosine-kinase inhibitors (TKI) compared to contrast-enhanced dual energy CT.

Materials and Methods

Patient population

This prospective study was approved by our institutional IRB and complies with HIPAA. In this study only patients that responded to therapy were included. Response was defined following RECIST criteria (absence of new lesions, reduction in SOL (sum of lesions) > 30%). A total of 26 patients diagnosed with mRCC (histological subtypes: 23 clear cell RCC; 3 papillary RCC) were included in this study. 19 males (mean age 61.4 ± 11.1 years) and 7 females (mean age 64.1 ± 15.7), all of them treated with TKIs (sunitinib), underwent venous phase DECT scans of the chest, abdomen and pelvis for staging or follow-up. Baseline scans were acquired within 7 days prior to the start of treatment with a TKI. Follow-up examinations were performed at 10 weeks, in the final week of the 2nd cycle of TKI administration. A total of 44 lesions were scanned for analysis.

Computed tomography

All scans were performed on a 128-slice dual-source CT scanner (Somatom Definition Flash, Siemens

Healthcare, Forchheim, Germany). Patients were scanned in the supine position. To ensure the patients´ central position within the field of view, two topograms (lateral and anterior-posterior) were acquired first. For all scans, 1.3 ml / kg bodyweight of nonionic iodinated contrast material (350 mg / ml iomeprol; Iomeron, Bracco, Milan, Italy) was injected intravenously with an automated dual-syringe power injector (Stellant D CT Injection System, MEDRAD, INC., Warrendale) at a flow rate of 2.5 ml / s and with a delay of 70 – 80 seconds. Subsequently patients were scanned in craniocaudal direction from the upper thoracic aperture to the pubic symphysis during inspiratory breath hold. Applied scanning parameters were 128 x 0.6 mm detector collimation and a pitch of 0.6. Tube voltages were 100 kVp for tube A and a tin-filtered 140 kVp for tube B. Gantry rotation speed was 0.5 seconds. Online dose modulation (Care-DOSE 4D, Siemens, Forchheim, Germany) was used. Radiation exposure was assessed for each patient using dose-length product (DLP).

Dual-Energy Post processing and Image Reconstruction

Using specific dual energy soft-tissue reconstruction kernels, contiguous axial slices with a slice thickness of 3 mm were reconstructed. Three different series of images can be generated from a dual energy dataset: 100 kVp images, 140 kVp images, and weighted-average images using 50% information from the high and low kVp dataset, respectively. On these “virtual 120 kVp“ images, contrast attenuation was measured. Images were loaded onto a dedicated DE postprocessing workstation (Syngo.via “CT Dual Energy“, Siemens Healthcare). Based on three-material decomposition principles, images from which iodine has been subtracted (VNE) as well images showing iodine related attenuation (IRA) can be calculated using an application called “Liver VNC“ [11]. By superimposing iodine-only images on VNE images, anatomical information and iodine distribution can be depicted simultaneously. These iodine overlay virtual images are largely equivalent to a standard contrast-enhanced CT image [15, 16].

Data Analysis

Circular regions of interest (ROIs) were placed on the iodine overlay images covering as much tissue of the analyzed RCC metastases as possible in order to provide representative measurements. Size and localization of these ROIs was kept as constant as possible for baseline and follow up examinations.

By drawing ROIs on iodine overlay images, density of the VNC image plus iodine density (which is called “venous“ density in this manuscript) and pure iodine density (ID) in HU as well as iodine concentration (IC in mg/ml) can be measured (Figure 1). To reduce the risk for measurement errors, two blinded radiologists independently defined ROIs for each lesion. The resulting mean value of these two measurements was used for further analysis.

Statistical Analysis

Normal distribution of the measured CT numbers was proven by Kolomogorov-Smirnov test. Means and standard deviations were calculated and results were tested for statistical significance by using Student two-tailed *t* test for paired samples. As statistical software MedCalc® (version 14.12.0, Mariakerke, Belgium) was used.

Results

Radiation exposure

Mean DLP was 838±414 mGy*cm for the baseline scans and 847±357 mGy*cm for the follow-up scans, $p>0.05$.

Quantitative evaluation of changes in tumor contrast enhancement

The graphs presented in figure 1 summarize venous and ID densities obtained from all analyzed lesions. Between baseline and follow-up examinations, venous dual energy CT density of all measured 44 lesions decreased from 76.7±17.7 HU to 53.1±17.3 HU ($p=0.001$), which equals a reduction in contrast enhancement of 29.5±20.8%. Mean ID for all lesions was 39.2±16.6 HU at baseline and 19.2±14.5 HU at follow-up examinations ($p<0.005$), respectively, representing a 49.8±36.3% reduction in contrast enhancement. Mean percentage decrease of ID was

significantly higher than that of venous dual energy CT numbers (p=0.0001).
Figure 2 shows iodine concentrations measured on the baseline examination compared to those found on the follow-up scans. IC decreased from 2.1±0.9 mg to 1.0±0.8 mg (p<0.001) which equals a percentage decrease of 50.7±39.9.

Discussion

In the treatment of mRCC, traditional approaches such as chemotherapy or radiation do not show clinically meaningful results. Moreover, many applied agents lead to severe toxic side effects [17, 18]. Only since antiangiogenic drugs are available for the therapy of mRCC and other highly perfused tumor entities, progression free survival as well as overall survival rates increased [19, 20]. New drug regimens require imaging specialists to reconsider traditional response imaging criteria: It is widely known that targeted therapies may lead to significant changes in contrast enhancement without showing a significant reduction in tumor size. Moreover, vascular effects of antiangiogenic therapy may occur long before a change in tumor size can be detected [21]. With the expensive TKI therapy an early prediction of response is eagerly needed. This is why novel response criteria in imaging, additional to tumor size, need to be defined. In highly vascularized tumors therapy response is marked by a decrease in tumor vessels [22]. In imaging, this devascularization is reflected by reduced contrast media uptake [23].
Therefore, visualizing and measuring contrast agent and differentiation of iodine uptake from underlying tissue density in a lesion is crucial for response imaging. DECT provides the opportunity to depict iodine uptake: through creating iodine maps pure iodine density without the underlying tissue density can be measured. With this information, changes in density due to (tumor) perfusion can be detected earlier, potentially increasing the sensitivity for tumor response or progression compared to multi-detector row computed tomography (MDCT).
As shown in this study, measuring pure iodine density or iodine concentration in lesions based on DECT iodine maps in mRCC shows significantly greater decrease of tumor vascularization due to antiangiogenic treatment than measuring venous density alone does.

Based on these results, it can be postulated that DECT will be more sensitive in the detection of subtle enhancement differences which may be useful in detection of early or subtle response to treatment.

These findings coincide with recently published DECT studies on other highly perfused tumor entities: Detecting iodine uptake of melanoma metastases in patients treated with targeted therapies adds important information for response imaging compared to RECIST alone [24]. For GIST, iodine related attenuation seems to be a more reliable response marker than Choi criteria [13, 14]. In hepatocellular carcinoma as well as in non-small cell lung cancer measuring iodine uptake is described to be an easily applicable, robust tool for therapy assessment [25, 26]. So far, DECT studies on renal tumors mainly focused on the characterization of renal masses rather than on assessment of response in metastatic disease [9, 27, 28, 29]. Therapy response studies on RCC are rare. Up to now there is only one published work describing the use of DECT for the assessment of therapy response after radiofrequency ablation without correlating these results to standard MDCT [30].

The results of this study need to be seen in light of the study design and its limitations. With 26 included subjects, the patient population is relatively small, although this still represents the largest population with mRCC undergoing DECT surveillance for treatment monitoring.

Furthermore, as patients did not undergo surgery during TKI therapy, tumorous tissue could not be harvested for correlation with histopathology or immune histochemical staining. Testing tissue samples e.g. for vessel density before and after treatment with TKI would serve as an ideal positive control for DECT findings, although this is only available in animal studies.

Images were acquired in venous phase only. Especially when looking at highly perfused tumour entities such as RCC, it seems to be preferable, if not necessary, to also perform arterial phase scans which would give additional information about tumor perfusion. On the other hand, as contrast media uptake in RCC metastases in the arterial phase is quite inhomogenous, reliable and reproducible measurements are hardly seen.

Yet, we do not know how well the observed decrease in tumor

vascularization after treatment with TKI correlates with patients´ clinical outcome (e. g. progression free survival, overall survival). To answer this question, large cohort follow-up studies are needed.

We have demonstrated that iodine density determined by DECT allows for significantly more sensitive detection of antiangiogenic treatment effects than contrast-enhanced dual energy CT and may serve as a new valid surrogate marker for response imaging in patients with mRCC on targeted therapy. It can be easily integrated into routine staging MDCT examinations without increasing the amount of contrast agent needed. As can be seen from the dose estimates (based on the DLP), no significant increase in radiation exposure compared to standard dose CT of the thorax, abdomen and pelvis was observed in our study population [31, 32]. On the contrary, as VNC images can be calculated from the DECT data set, additional non-enhanced scans (e. g. to differentiate intratumoral hemorrhage from an enhancing lesion) might not be necessary anymore. We reveal that DECT in response imaging has great potential for mRCC under TKI therapy as well as other tumor entities. To confirm the results of this work additional DECT studies including higher numbers of patients with mRCC or other highly perfused tumor entities undergoing targeted therapies need to be performed.

This study demonstrates for the first time that response imaging in mRCC is feasible using DECT and, moreover, that DECT is even more sensitive to antiangiogenetic therapy induced changes in tumor vascularization than contrast-enhanced dual energy CT. Further studies are warranted to show the potential of this technology in the differentiation of responders from non-responders.

Tables and Figures

FIGURE 1. Venous/CT densities (grey) and iodine densities (blue) of all lesions Compared to baseline (BL) a 29.5 % reduction in contrast media uptake can be found in the follow-up (FU) examinations for venous CT. An even stronger decrease in iodine enhancement was found for ID: -49.8 % in between BL and FU

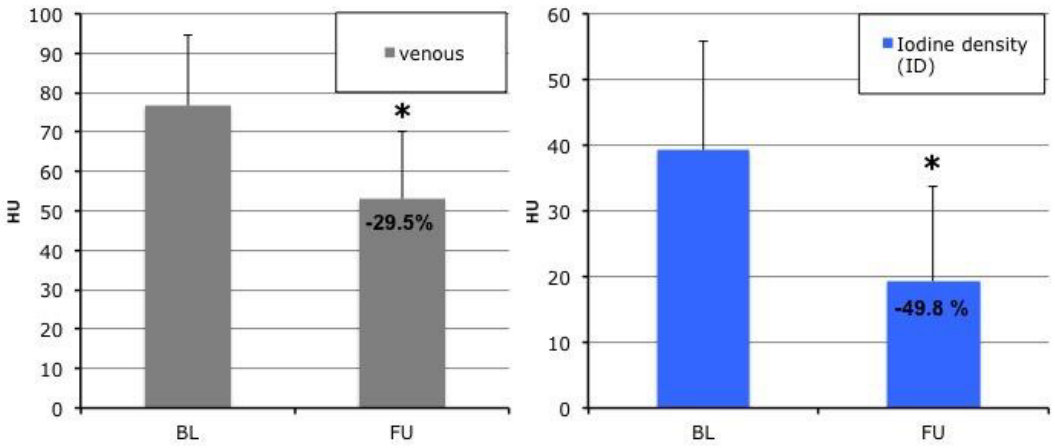

FIGURE 2. Iodine concentrations of all lesions at baseline (BL) and follow-up (FU) IC showed a 50.7 % decrease in between BL and FU

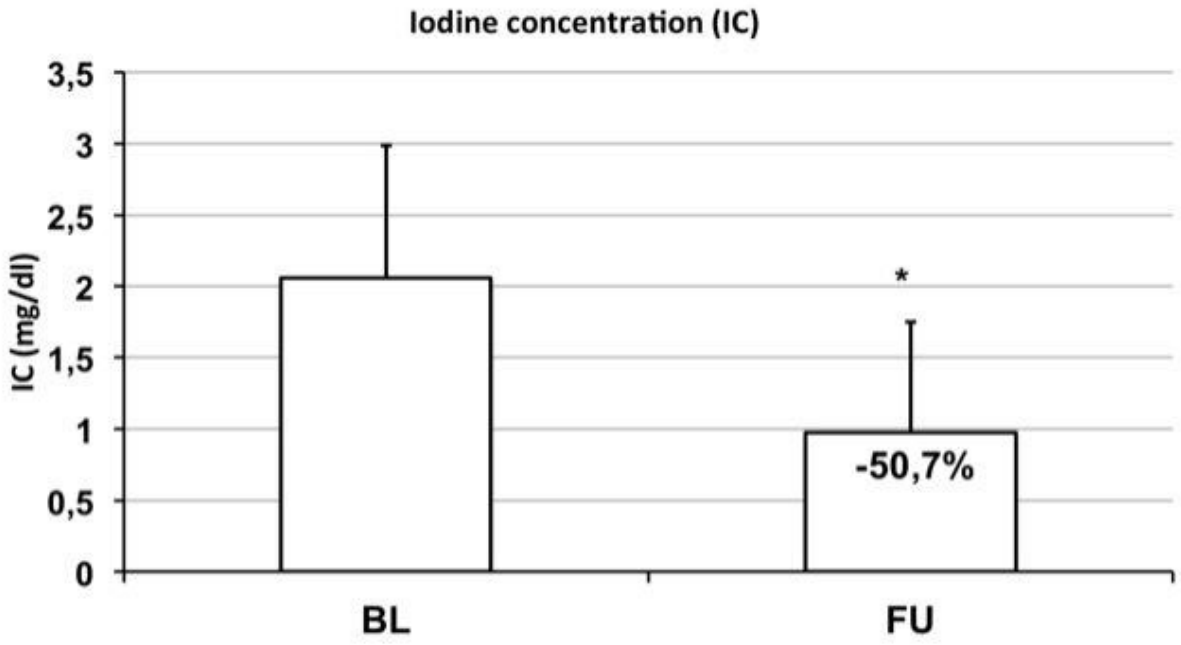

FIGURE 3. Visualizing contrast media uptake using DECT. Figure 3 gives an example of DECT contrast media enhancement in RCC metastases before (a, c) and ten weeks after the beginning of TKI therapy (b, d). Contrast media uptake is encoded in red. By placing ROIs in the lesions, venous dual energy CT density, ID and IC can be measured. Both follow-up examinations show a strong decrease of density in the venous phase, which is 25 HU (-37.7 %) for the lesion located in the left adrenal gland (a, b) and 16 HU (-36.4 %) for pelvic osseous metastases (c, d). An even larger reduction in contrast media enhancement can be observed for ID: The difference between baseline and follow-up is 24 HU (-55.8 %) measured in the adrenal gland lesion and 13 HU (-62.9 %) for the soft tissue component of the bone metastasis. Accordingly, IC showed a similar degree of reduction in iodine concentration (metastasis adrenal gland: 1.3 mg/ml, -56.5 %; pelvic lesion 0.8 mg/ml, -66.7 %)

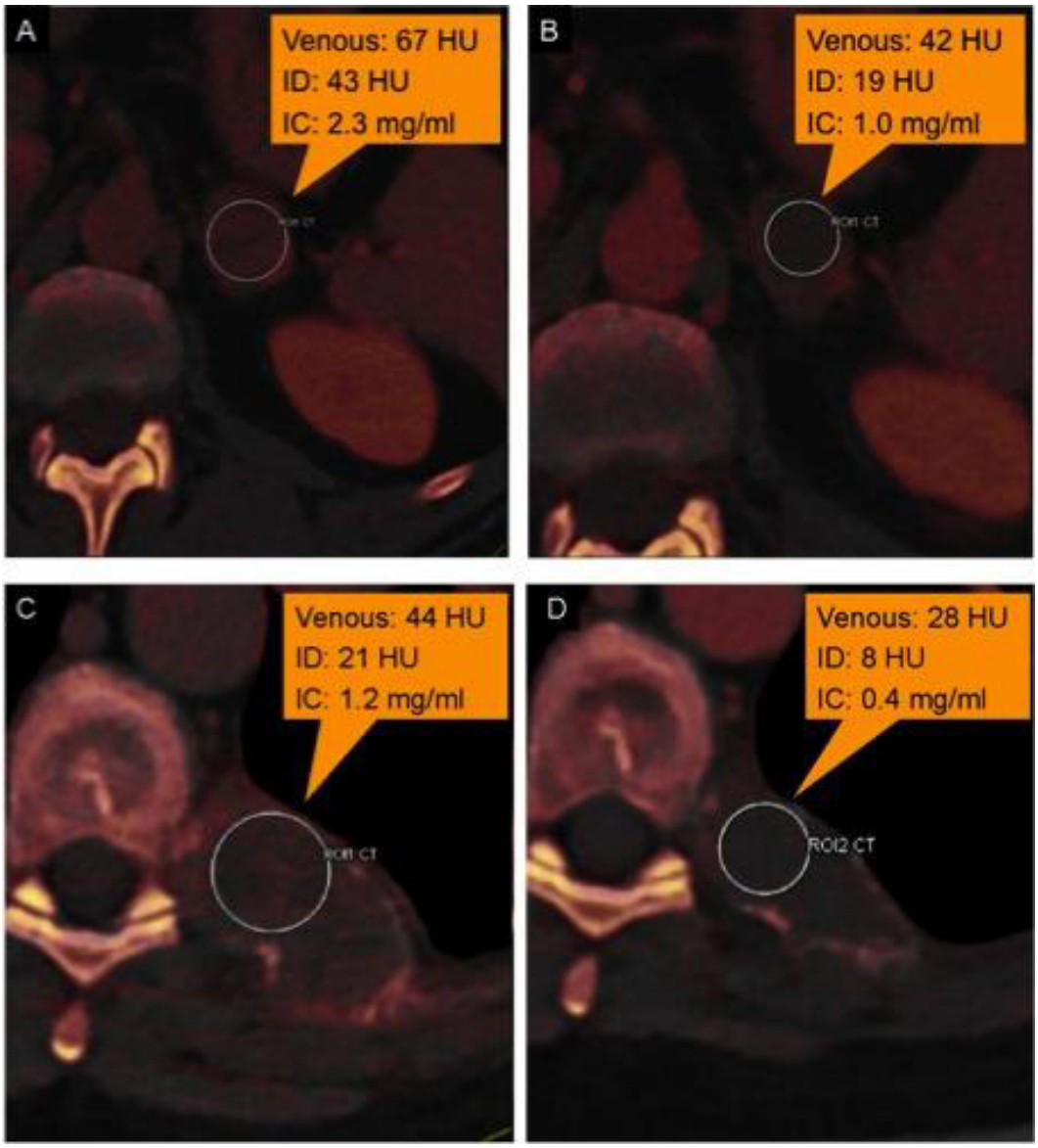

References

1. Gupta K, Miller JD, Li JZ, Russell MW, Charbonneau C (2008) Epidemiologic and socioeconomic burden of metastatic renal cell carcinoma (mRCC): a literature review. Cancer Treat Rev 34:193-205
2. Janzen NK, Kim HL, Figlin RA, Belldegrun AS (2003) Surveillance after radical or partial nephrectomy for localized renal cell carcinoma and management of recurrent disease. Urol Clin North Am 30:843-852
3. Ljungberg B, Campbell SC, Choi HY et al (2011) The epidemiology of renal cell carcinoma. Eur Urol 60:615-621
4. Athar U, Gentile TC (2008) Treatment options for metastatic renal cell carcinoma: a review. Can J Urol 15:3954-3966
5. Aslam S, Eisen T (2013) Vascular endothelial growth factor receptor tyrosine kinase inhibitors in metastatic renal cell cancer: latest results and clinical implications. Ther Adv Med Onco l5:324-333
6. Eisenhauer EA, Therasse P, Bogaerts J et al (2009) New response evaluation criteria in solid tumours: revised RECIST guideline (version 1.1). Eur J Cancer 45:228-47
7. Brufau BP, (2013) Metastatic renal cell carcinoma: radiologic findings and assessment of response to targeted antiangiogenic therapy by using multidetector CT. Radiographics 33:1691-1716
8. Choi H, Cerqueda CS, Villalba LB, Izquierdo RS, Gonzales BM, Molina CN (2008) Response evaluation of gastrointestinal stromal tumors. Oncologist 13 Suppl 2:4-7
9. Graser A, Becker CR, Staehler M (2010) Single-phase dual-energy CT allows for characterization of renal masses as benign or malignant. Invest Radiol 45:399-405
10. Johnson, TR (2012) Dual-energy CT: general principles. AJR. Am J Roentgenol 199: S3-8
11. Graser A, Johnson TR, Chandarana H, Macari M (2009) Dual energy CT: preliminary observations and potential

clinical applications in the abdomen. Eur Radiol 19:13-23

12. Lee JA, Jeong WK, Kim Y (2013) Dual-energy CT to detect recurrent HCC after TACE: initial experience of color-coded iodine CT imaging. Eur J Radiol 82:569-576
13. Apfaltrer P, Meyer M, Meier C et al (2012) Contrast-enhanced dual-energy CT of gastrointestinal stromal tumors: is iodine-related attenuation a potential indicator of tumor response? Invest Radiol 47:65-70
14. Meyer M, Hohenberger P, Apfaltrer P et al (2013) CT-based response assessment of advanced gastrointestinal stromal tumor: dual energy CT provides a more predictive imaging biomarker of clinical benefit than RECIST or Choi criteria. Europ J Radiol 82:923-928
15. Tawfik AM, Kerl JM, Razek AA (2011) Image quality and radiation dose of dual-energy CT of the head and neck compared with a standard 120-kVp acquisition. AJNR Am J Neuroradiol 32:1994-9
16. Stiller W, Schwarzwaelder CB, Sommer CM, Veloza S, Radeleff BA, Kauczor HU (2012) Dual-energy, standard and low-kVp contrast-enhanced CT-cholangiography: a comparative analysis of image quality and radiation exposure. Eur J Radiol 81:1405-12
17. Atzpodien J, Schmitt E, Gertenbach U et al (2005) Adjuvant treatment with interleukin-2- and interferon-alpha2a-based chemoimmunotherapy in renal cell carcinoma post tumour nephrectomy: results of a prospectively randomised trial of the German Cooperative Renal Carcinoma Chemoimmunotherapy Group (DGCIN). Br J Cancer 92:843-846
18. Hudes G, Carducci M, Tomczak P et al (2007) Temsirolimus, interferon alfa, or both for advanced renal-cell carcinoma. N Engl J Med 356:2271-2281
19. Jonasch E, Corn P, Pagliaro LC et al (2010) Upfront, randomized, phase 2 trial of sorafenib versus sorafenib and low-dose interferon alfa in

patients with advanced renal cell carcinoma: clinical and biomarker analysis. Cancer 116:57-65

20. Motzer RJ, Rini BI, Bukowski RM et al (2006) Sunitinib in patients with metastatic renal cell carcinoma. JAMA 295:2516-2524
21. Bex A, Fournier L, Lassau N et al (2014) Assessing the response to targeted therapies in renal cell carcinoma: technical insights and practical considerations. Eur Urol 65:766-777
22. Choueiri TK (2011) VEGF inhibitors in metastatic renal cell carcinoma: current therapies and future perspective. Curr Clin Pharmacol 6:164-168
23. Lv P, Liu J, Yan X et al. (2016) CT spectral imaging for monitoring the therapeutic efficacy of VEGF receptor kinase inhibitor AG-013736 in rabbit VX2 liver tumours. Eur Rad (epub ahead of print)
24. Uhrig M, Sedlmair M, Schlemmer HP, Hassel JC, Ganten M (2013) Monitoring targeted therapy using dual-energy CT: semi-automatic RECIST plus supplementary functional information by quantifying iodine uptake of melanoma metastases. Cancer Imaging 13:306-313
25. Dai X, Schlemmer HP, Schmidt B et al (2013) Quantitative therapy response assessment by volumetric iodine-uptake measurement: initial experience in patients with advanced hepatocellular carcinoma treated with sorafenib. Eur J Radiol 82:327-334

26 Baxa J, Matouskova T, Krakorova G et al. (2015) Dual-Phase Dual-Energy CT in Patients Treated with Erlotinib for Advanced Non-Small Cell Lung Cancer: Possible Benefits of Iodine Quantification in Response Assessment. Eur Radiol [Epub ahead of print]

27. Song KD, Kim CK, Park BK, Kim B (2011) Utility of iodine overlay technique and virtual unenhanced images for the characterization of renal masses by dual-energy CT. AJR 197:1076-1082
28. Helck A, Hummel N, Meinel FG, Johnson T, Nikolaou K, Graser A et al (2014) Can single-phase

dual-energy CT reliably identify adrenal adenomas? Eur Radiol 24:1636-1642

29. Mileto A, Sofue K, Marin D (2016) Imaging the renal lesion with dual-energy multidetector CT and multi-energy applications in clinical practice: what can it truly do for you? Eur Radiol (epub ahead of print)
30. Park SY, Kim CK, Park BK (2014) Dual-energy CT in assessing therapeutic response to radiofrequency ablation of renal cell carcinomas. Eur J Radiol 83:73-79
31. Tsapaki V, Aldrich JE, Sharma R et al. (2006) Dose reduction in CT while maintaining diagnostic confidence: diagnostic reference levels at routine head, chest, and abdominal CT--IAEA-coordinated research project. Radiology 240:828-34
32. Wichmann JL, Hardie AD, Schoepf UJ et al (2016) Single- and dual-energy CT of the abdomen: comparison of radiation dose and image quality of 2nd and 3rd generation dual-source CT. Eur Radiol (epub ahead of print)